13,14

On the power law distributions of local stresses and strains in the fracture process of heterogeneous materials revealed via discrete element method

© V.L. Hilarov, E.E. Damaskinskaya

Ioffe Institute,
St. Petersburg, Russia

E-mail: Vladimir.Hilarov@mail.ioffe.ru

Received January 15, 2025
Revised January 21, 2025
Accepted January 22, 2025

Distributions of local tensile stresses and strains in the fracture process of heterogeneous materials are studied by means of the discrete element method. Local stresses here are stresses on bonds in the bonded particle model. It is shown that these distributions become wider as the fracture process evolves. The approximation of long-wave tails by exponential and power functions is carried out, and the change in time of these function parameters is calculated.

Keywords: Fracture of heterogeneous materials, discrete element method, stress and strain distributions.

DOI: 10.61011/PSS.2025.02.60690.10-25

1. Introduction

Power series distributions of quantities in physical systems usually occur in critical situations such as phase transitions [1], percolation threshold [2], self-organized criticality state [3]. Such distributions are also observed in the physics of fracture of mechanically loaded materials: for example, a well-known Gutenberg-Richter law, acoustic emission (AE) signal distribution over energies on approach to material fracture [4], and size distribution of load-induced defects [5].

This study investigates the distribution of bonds over strains and stresses, and correlations thereof. Calculations were conducted by the discrete element method in a bonded particle model (BPM) proposed in [6]. The simulation experiments were carried out in MUSEN freeware package [7].

2. Description of the computer experiment

Cylindrical samples 10 mm in diameter and 20 mm in height were simulated. A sample was placed into a virtual press. The lower plate was fixed and the upper plate moved down at a constant speed of $v = 0.02$ m/s. Thus, uniaxial compression was simulated. The experiment setup is similar to that described in [8].

Two sets of samples were studied. Samples from Set 1 contained 48,695 spherical particles with diameters and content as specified in Table 1. Particle sizes are a set of sizes with a mean value of 0.3 mm and a standard deviation of 0.1 mm, which was obtained by a normal random number generator.

Sample set 2 contained 33670 spherical particles with diameters and content as specified in Table 2. These sizes are a set of sizes with a mean value of 0.08 mm and a standard deviation of 0.025 mm which was obtained by a normal random number generator. Grain diameter 4 for orthoclase is increased by an order of magnitude to improve the degree of heterogeneity.

Physical properties of materials for particles and bonds were chosen from Table 3.

A total of 9 samples with bond parameters from Table 4 were examined. Three types of bonds between particles: type 1 corresponded to orthoclase bonds, type 2 corresponded to the case when particles of one material were

Table 1. Grain diameters (mm) and percentage composition of each of the fractions

	Grain diameter of various fractions d_i, mm					Content of each fraction
Quartz	0.36	0.188	0.52	0.28	0.42	0.0595745
Orthoclase	0.27	0.28	0.4	0.36	0.26	0.0702128
Oligoclase	0.16	0.168	0.288	0.24	0.4	0.0702128

Table 2. Grain diameters (mm) and percentage composition of each of the fractions

	Grain diameter of various fractions d_i, mm					Content of each fraction
Quartz	0.09	0.047	0.132	0.079	0.106	0.0595745
Orthoclase	0.068	0.07	0.096	0.91	0.064	0.0702128
Oligoclase	0.041	0.042	0.077	0.063	0.098	0.0702128

Table 3. Properties of materials used for simulation

№	Material	ρ, kg/m^3	E, GPa	ν	σ_n, MPa	σ_t, MPa	η, Pa·s
1	quartz	2650	94	0.29	600	600	5E19
2	Orthoclase	2560	62	0.29	420	420	1E19
3	Oligoclase	2560	70	0.29	480	480	1E19
4	Glass	2500	50	0.22	50	50	1E40
5	Quartz-orthoclase bond	2500	5.8	0.2	200	200	5E19
6	Quartz-oligoclase bond	2500	5.8	0.2	300	300	5E19
7	Orthoclase-oligoclase bond	2500	5.8	0.2	100	100	5E19

Note. ρ is the material density, E is Young's modulus,ν is Poisson's ratio, σ_n is the tensile strength of the material, σ_t is the shear strength of the material, η is the dynamic viscosity.

Table 4. Bond parameters

Sample №	1	2	3	4	5	6	7	8	9
Number of bonds	33670	33670	48695	48695	48695	48695	48695	48695	33670
Type of bonds	1	1	1	1	2	3	3	3	3
Bond diameter (mm)	$d = 0.04$	$d \leq 0.1$	$d = 0.1$	$d \leq 0.6$	$d \leq 0.6$	$d \leq 0.2$	$d = 0.1$	$d \leq 0.6$	$d \leq 0.1$

bound by the same material, and particles from different materials were linked by low-modulus bonds 5–7 (Table 3). Type 3 corresponded to a case when particles of the same material were bound by the same material, while particles of different materials were linked by brittle glass bonds (Table 3).

During the fracture process, a large set of various physical properties of samples was recorded in equal time intervals (data storage interval) to be used for future analysis. As such properties, this study used distributions of tension strains and stressed on bonds over their magnitudes.

3. Computer simulation data and discussion

Long-wavelength tails of stress and strain distributions obtained by computer simulation at each time step were approximated by exponential and power functions because these particular functions are responsible for the Markovian short-memory processes (exponent) and scaling (power function) that occurs in critical states (phase transitions, self-organized criticality, etc.). Approximation quality was assessed by the coefficient of determination R^2. As an example, Figure 1 shows typical dependences of these coefficients on time for sample № 5 (stress distribution).

It can be seen that the exponential function adequately describes the distribution throughout the process. The power function describes the process a little worse in the beginning (but also adequately, $R^2 > 0.93$), but is better than the exponential approximation at the end of the process, which is typical for the self-organized criticality process. Time dependences R^2 also have the same form for other samples.

As scaling coefficients (power exponents) are of foremost interest, they will be addressed hereinafter. Figure 2 shows loading diagrams and time dependences of scaling variables for samples 4, 5 and 8 having the same grain and bond sizes, but different types of bonds (Table 4 and the description).

It is shown that stress and strain distributions generally broaden as the system approaches its fracture. Some details may be understood from the loading diagram and bond fracture kinetics in these samples as shown in Figure 3.

Thus, saturation of the dependences in Figure 2, d–f at $t \approx 0.088$ s is associated with depletion of „glass" bond fractures and low fracture rate of other bonds. The maximum of dependence in Figure 2, g–i for the stress scaling coefficient at $t \approx 0.02$ s may be understood, if a time dependence of the stress scaling coefficient is built for each

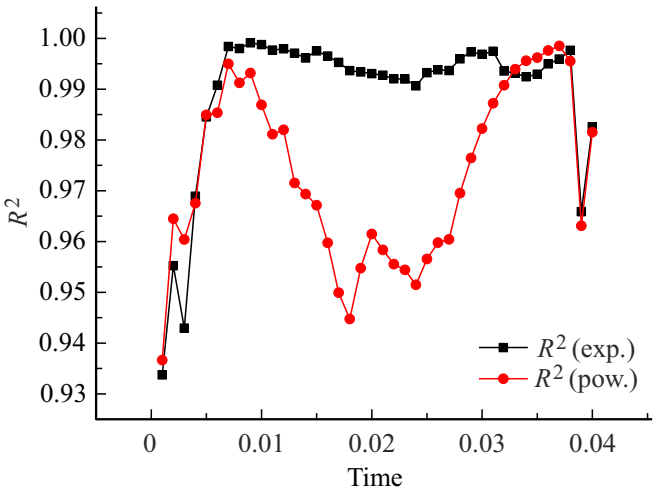

Figure 1. Coefficients of determination in the approximation of dependence of stress distribution on time in sample №5.

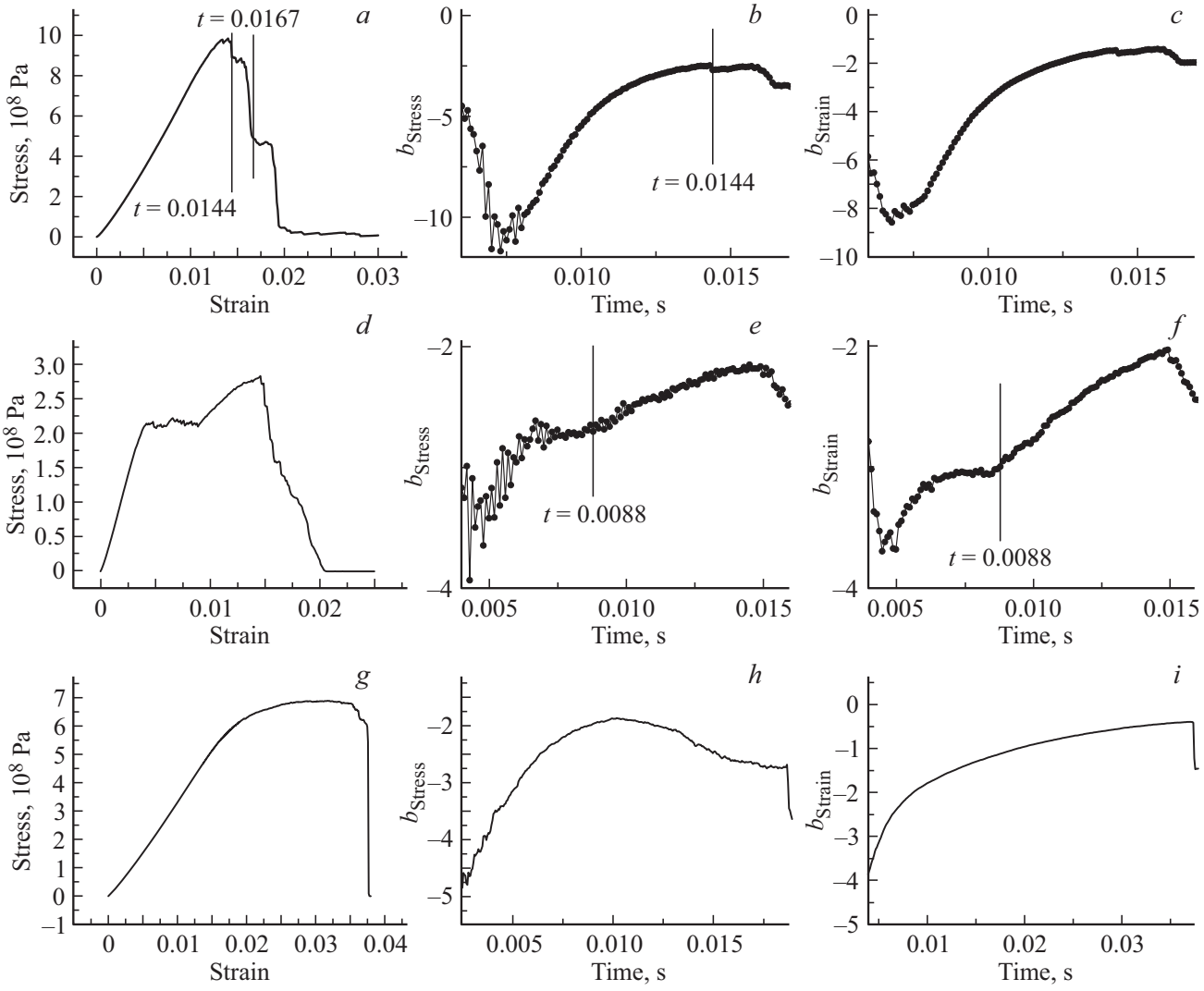

Figure 2. Loading diagram, time dependence of scaling coefficient for stresses (b_{stress}) and strains (b_{strain}) for the sample with orthoclase bonds 48695 $d \leq 0.6$ (a–c), for the sample with glass bonds (d–f) and for the sample with low-modulus bonds (g–i).

type of bonds existing in this material (Figure 4). According to these curves, distributions for individual types of bonds also broaden on the approach to fracture for all types of bonds, except 7 (orthoclase–oligoclase). (For bond type 7, the power approximation appears to be inadequate in a considerable time region). This maximum occurs because „intergranular bonds" (i. e. low-modulus bonds between particles of different materials) begin to fracture much later than „intragranular" bonds (i. e. bonds between particles of the same material) and variation of the scaling coefficient at $t \approx 0.02$ s is irregular. Thus, it has an artifact form. Distribution of strains for this sample keeps on broadening because its power exponent decreases monotonously.

Correlation coefficients of strain and stress scaling coefficients for all studied samples ($\rho_{\sigma\varepsilon}$) are shown in Table 5.

As it follows from Table 5, the highest correlation coefficients are observed for more homogeneous samples (1–4) with one type of orthoclase bonds. Such samples are elastically strained to fracture (brittle fracture), therefore observance of Hooke's law in them ensures strong correlations between stresses and strains (Figure 2, a–c). Less significant correlations are observed for samples with glass bonds (7–9). In this case, increased heterogeneity is caused by lower (by an order of magnitude) strength of glass bonds with a slight difference in their modules from other bonds. Hooke's law is satisfied until start of fracture. After fracture of almost all bonds, Hooke's law becomes true again because they are still able to be elastically strained

Table 5. Correlation coefficients of strain and stress scaling coefficients

Sample	1	2	3	4	5	6	7	8	9
$\rho_{\sigma\varepsilon}$	0.971	0.967	0.921	0.994	0.644	0.845	0.835	0.846	0.815

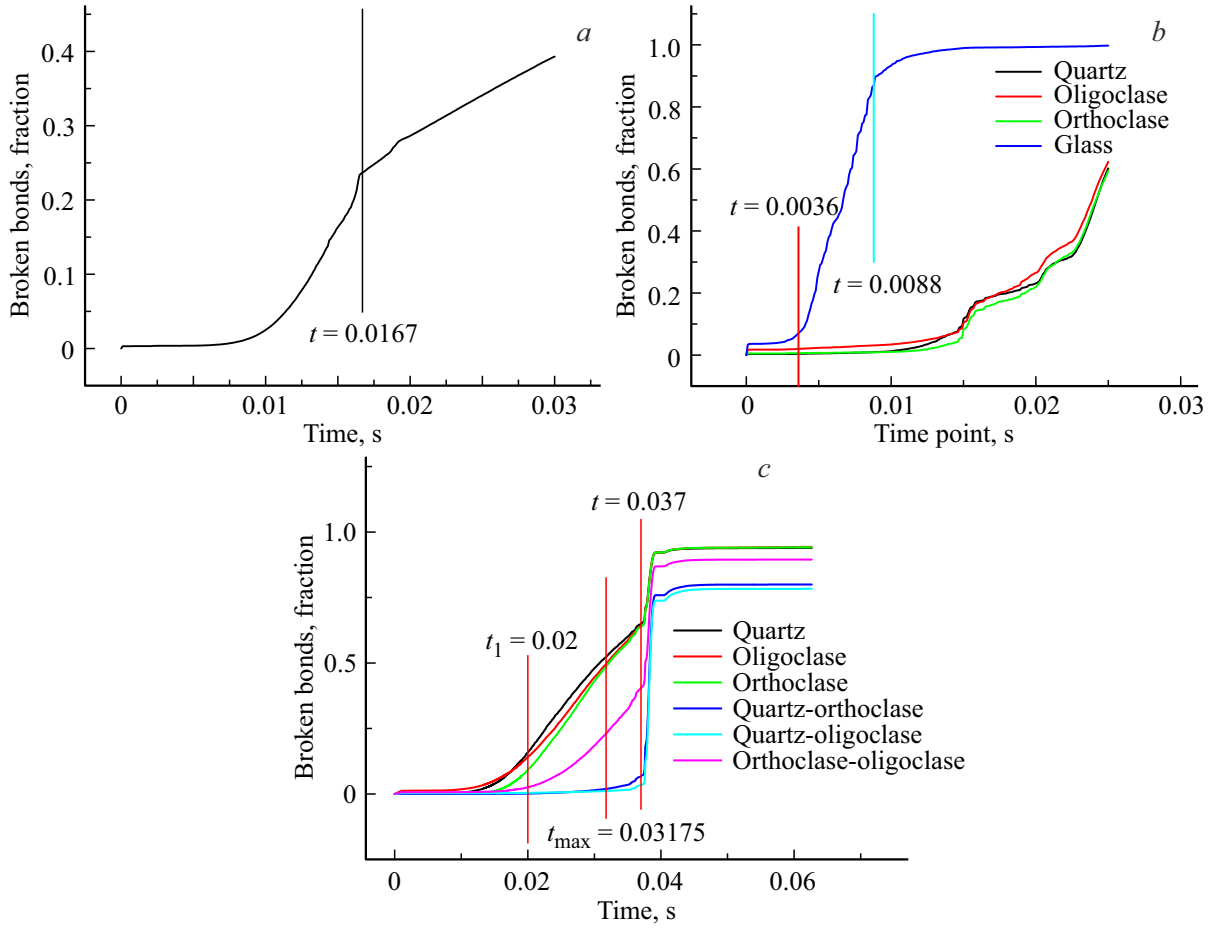

Figure 3. Bond fracture kinetics in samples 4 (*a*), 8 (*b*) and 5 (*c*).

due to a higher strength of other bonds. For the sample with low-modulus bonds (5), the correlation coefficient is even low.

Correlation coefficients between the maximum power exponents (critical indices [1]) were calculated before fracture for all studied materials. Correlations between strain and stress indices (-0.601) appeared to be low. Such relations between distribution widths may be explained by the fact that, as established in [8], structural inhomogeneity gives rise to a higher stress homogeneity (multiplicity of areas with higher stresses) and, conversely, fracture of more homogeneous materials is induced by a single site (crack). Considerable spread of critical indices don't allow to assert definitely that they don't depend on the physical nature of material.

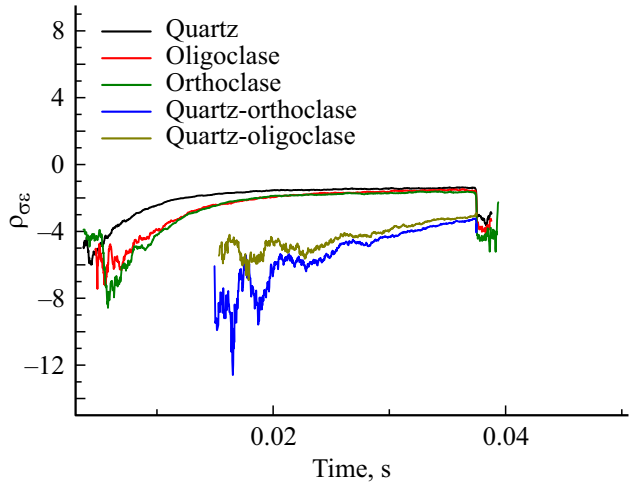

Figure 4. Time dependence of stress scaling coefficient for a sample with low-modulus bonds.

4. Conclusion

Thus, it is shown that bond strain and stress distributions broaden during material deformation and become power functions. Correlation coefficients of time dependences of strain and stress scaling coefficients are defined by correspondence of $\sigma(\varepsilon)$ to Hooke's law. Correlation coefficients of the critical indices (maximum scaling coefficients) are associated with material heterogeneity (in terms of structure or internal stresses). The maximum value (minimum absolute value) is achieved before the fracture time.

Formation of power series distributions before fracture of a material reflects a scale invariance of physical systems in critical state, which, in our opinion, is the implementation of the self-organized criticality process in case of fracture.

Funding

The study was performed under state assignment of Ioffe Institute.

Conflict of interest

The authors declare that they have no conflict of interest.

References

[1] R. Balesku. Ravnovesnaya i neravnovesnaya statisticheskaya mekhanika. V. 1. Mir, M. (1978). 408 s. (in Russian).
[2] Kh. Guld, Ya. Tobochnik. Komp'yuternoye modelirovaniye v fizike. V. 2. Mir, M. (1990). p. 390. (in Russian).
[3] D. Marković, C. Gros. Phys. Rep. **536**, *2*, 41 (2013).
[4] E. Damaskinskaya, D. Frolov, D. Gafurova, D. Korost, I. Panteleev. Interpretation **5**, *4*, SP1 (2017).
[5] E.E. Damaskinskaya, V.L. Gilyarov. FTT **66**, 142 (2024). (in Russian).
[6] D.O. Potyondy, P.A. Cundall. Int. J. Rock Mech. Min. Sci. **41**, 1329 (2004).
[7] M. Dosta, V. Skorych. Software **X12**, 100618 (2020).
[8] V.L. Gilyarov, E.E. Damaskinskaya. FTT **64**, 676 (2022). (in Russian).

Translated by E.Ilinskaya